CROMER, D. T. (1974). *International Tables for X-ray Crystallography*, Vol. IV, pp. 148–151. Birmingham: Kynoch Press. (Present distributor Kluwer Academic Publishers, Dordrecht.) The tabulated f' values need to be adjusted by wavelength-independent corrections given by KISSEL, L. & PRATT, R. H. (1990). *Acta Cryst.* A**46**, 170–175.
CRUICKSHANK, D. W. J. (1949). *Acta Cryst.* **2**, 65–82.
DETITTA, G. T. (1985). *J. Appl. Cryst.* **18**, 438–440.
FRENCH, S. & WILSON, K. (1978). *Acta Cryst.* A**34**, 517–525.
HANSEN, N. K. & COPPENS, P. (1978). *Acta Cryst.* A**34**, 909–921.
HERMANSSON, K. (1984). *Acta Universitatis Upsaliensis*, p. 744. Doctoral Dissertation, Univ. of Uppsala.
MOSS, G. R., SOUHASSOU, M., ESPINOSA, E., LECOMTE, C. & BLESSING, R. H. (1995). *Acta Cryst.* B**51**, 650–660.
NELMES, R. J. (1975). *Acta Cryst.* A**31**, 273–279.
O'KEEFE, M., DOMENGÈS, B. & GIBBS, G. V. (1985). *J. Phys. Chem.* **89**, 2304–2309.
STEWART, R. F., DAVIDSON, E. R. & SIMPSON, W. T. (1965). *J. Chem. Phys.* **42**, 3175–3187.
ZACHARIASEN, W. H. (1967). *Acta Cryst.* **23**, 558–564.

Acta Cryst. (1995). B**51**, 668–673

Crystal Structure of the Antiferroelectric Perovskite Pb_2MgWO_6

BY G. BALDINOZZI AND PH. SCIAU*

Laboratoire de Chimie-Physique du Solide, URA CNRS 453, Ecole Centrale Paris, 92295 Châtenay-Malabry CEDEX, France

M. PINOT

Laboratoire Léon Brillouin, CEA-CNRS, CEN Saclay, 91191 Gif-sur-Yvette CEDEX, France

AND D. GREBILLE

Laboratoire CRISMAT, ISMRA, Bd du Maréchal Juin, 14050 Caen CEDEX, France

(*Received* 25 *July* 1994; *accepted* 1 *December* 1994)

Abstract

Lead magnesium tungstate, Pb_2MgWO_6, M_r = 718.54. Phase I: cubic, Z = 4, $Fm3m$, a = 8.0058 (4) Å, V = 513.1 (2) Å^3, D_x = 9.30 Mg m^{-3} at 350 K, final R_{wp} = 4.5 and 7.7%, R_{Bragg} = 2.9 and 5.7% for neutron and X-ray powder data, respectively. Phase II: orthorhombic, $Pmcn$ ($Pnma$), Z = 4, a = 7.9440 (4) and 7.9041 (3), b = 5.6866 (3) and 5.7035 (2), c = 11.4059 (5) and 11.4442 (4) Å, V = 515.3 (1) and 515.9 (1) Å^3 at 294 and 80 K, respectively, D_x = 9.26 Mg m^{-3} at 294 K. Final R_{wp} = 4.0 and 8.5%, R_{Bragg} = 4.0 and 9.2% at 294 K and R_{wp} = 4.0 and 7.4%, R_{Bragg} = 2.9 and 8.4% at 80 K for neutron and X-ray powder data, respectively. To achieve the determination of the structures, X-ray and neutron powder diffraction data were refined together using the Rietveld profile method. The Pb main displacement in the orthorhombic phase from the ideal cubic positions is almost along the $[012]_o$ direction. The O displacements correspond to a weak distortion of the octahedra.

Introduction

The ideal structure of perovskite-type oxide compounds (ABO_3, space group $Pm3m$) is well known and very simple. Its prototype is $CaTiO_3$. It consists of tetravalent B cations at the center of corner-sharing oxygen octahedra, at the cubic cell origin for example, and divalent A cations at the cell center. In the general family of lead-based perovskites, various compounds have been synthesized by occupying the B site by two species of cation (Galasso, 1990). This leads to the general formula $Pb_2B'_xB''_{1-x}O_6$. Depending on ionic radii and charges, ordering of cations may occur, giving rise to different structural characteristics (different types of superstructure cells, for example) and to various very selective physical properties. The prototype structure of the totally ordered materials consists of a cubic cell with a doubled parameter around 8 Å, and of a centered space group $Fm3m$ resulting from the alternation of cations B' and B''. These perovskite oxides often have very large dielectric permittivities. The degree of long-range order between the species B' and B'' induces different behavior as a function of temperature. Partially or fully disordered compounds exhibit diffuse transitions and relaxor phenomena which are adequate for technological applications (capacitors, actuators, etc.). Ordered compounds present sharper transitions and their sequence of phase transitions is also strongly dependent on the cations involved.

The ordered complex perovskite Pb_2MgWO_6 (PMW) is quite interesting. It undergoes a first-order phase transition from the cubic phase ($Fm3m$) to an orthorhombic antiferroelectric phase at 312 K (Smolenskii, Krainik & Agranovskaya, 1961). The low-temperature phase is

* Author to whom correspondence should be addressed.

very close to the orthorhombic phase (III) of Pb_2CoWO_6 (Baldinozzi, Sciau & Buffat, 1993; Choo, Kim, Yang, Lim, Lee, Kwon & Chun, 1993). The latter compound is the subject of many investigations because of the complex phase sequence with an incommensurate phase (II). The structural determination of the orthorhombic phase of PMW can supply information on phase III of Pb_2CoWO_6 (PCW). On the other hand, PMW is the end member of the solid–solution series, as $PbMg_{1/2}W_{1/2}O_3$–$PbMg_{1/3}Nb_{2/3}O_3$, $PbMg_{1/2}W_{1/2}O_3$–$PbFe_{1/2}Ta_{1/2}O_3$ or $PbMg_{1/2}W_{1/2}O_3$–$PbFe_{1/2}Nb_{1/2}O_3$, which are interesting from a fundamental and a practical point of view because of the relaxor effect (Smolenskii *et al.*, 1961; Uchino & Nomura, 1976; Lee & Choo, 1981).

In a recent paper (Baldinozzi *et al.*, 1993) the space group *Pmcn* was determined and a structural model was proposed for the orthorhombic phase. In this paper we present a detailed structural determination carried out by X-ray and neutron powder diffraction.

Experimental

Pb_2MgWO_6 powder samples were prepared by the usual solid-state reaction from stoichiometric quantities of reagents: PbO, MgO and WO_3 (Tokmyanina, Razumovskaya & Belyaev, 1976).

X-ray powder patterns were collected up to $\sin(\theta_{max})/\lambda = 0.69$ Å^{-1} on a high-accuracy Microcontrole diffractometer, using Cu $K\beta$ radiation (graphite monochromator) and a rotating anode generator of 18 kW. The records (350, 294 and 80 K) were perfomed in a flowing cryostat (stability 0.1 K). Data collection conditions have been optimized in order to improve the peak-to-background ratio.

The neutron powder diffraction pattern was collected at the same temperatures on the high-resolution powder diffractometer 3T2 [$\lambda = 1.225$ Å and $\sin(\theta_{max})/\lambda = 0.67$ Å^{-1}] at Laboratoire Léon Brillouin.

Structural refinements were carried out using the Rietveld profile method by means of an *XND* computer program (Bérar & Garnier, 1992). Neutral atomic scattering factors taken from *International Tables for X-ray Crystallography* (1974, Vol. IV) and neutron-scattering lengths 9.4017, 5.375, 4.77 and 5.803 fm for Pb, Mg, W and O atoms, respectively, were used.

Refinement

To achieve a better determination of the structure, X-ray and neutron powder diffraction data were refined together.* This process presents the advantage of using the complementary specifications of neutron and X-ray data. The structural and instrumental parameters are better separated. The correlations between refined parameters are significantly reduced.

Table 1. *Results of refinement in the cubic phase at 350 K*

		(*a*)	(*b*)	(*c*)	(*d*)	(*e*)
Pb	*x*	1/4	1/4	0.2785 (7)	0.2729 (7)	0.257 (3)
	y	1/4	1/4	1/4	0.2729 (7)	0.257 (3)
	z	1/4	1/4	1/4	1/4	0.257 (3)
	B (Å^2)	2.87 (2)	2.83 (2)	1.3 (2)	0.9 (2)	2.6 (2)
Δ(Pb) Å				0.228 (10)	0.259 (8)	0.10 (4)
Mg	*B*	0.69 (4)	0.65 (3)	0.64 (3)	0.63 (3)	0.66 (3)
W	*B*	0.57 (3)	0.55 (3)	0.53 (3)	0.51 (3)	0.53 (3)
O	*x*	0.2397 (1)	0.2398 (1)	0.2398 (1)	0.2398 (1)	0.2398 (1)
	y	0	0.0221 (8)	0.0214 (10)	0.0229 (7)	0.0221 (8)
	z	0	0.007 (3)	0.009 (3)	0.004 (5)	0.007 (3)
	B	1.40 (2)	0.45 (3)	0.42 (3)	0.41 (3)	0.45 (3)
Δ(O) Å			0.186 (6)	0.186 (7)	0.186 (6)	0.186 (6)
R factor		*XR* *N*	*XR* *N*	*XR* *N*	*XR* *N*	*XR* *N*
R_{wp} (%)		7.9 5.6	7.8 4.5	7.7 4.5	7.7 4.5	7.8 4.5
R_{wp-c}		19.2 16.3	18.5 12.3	18.4 12.2	18.3 12.1	18.5 12.3
R_B		6.2 4.7	5.8 3.1	5.8 3.0	5.7 2.9	5.9 3.1

(*a*) All atoms on special position, (*b*) O-shifted, (*c*), (*d*) and (*e*). O-shifted and Pb along the ⟨100⟩, ⟨110⟩ and ⟨111⟩ directions, respectively.

Structure of the cubic phase

We have already indicated that the diffraction pattern above 312 K can be indexed in a cubic symmetry with a cell parameter of *ca* 8 Å in the *Fm3m* space group. In a first step, the atoms were fixed on their special positions, *i.e.* Pb (8*c*) ($\frac{1}{4},\frac{1}{4},\frac{1}{4}$), Mg (4*b*) ($\frac{1}{2},\frac{1}{2},\frac{1}{2}$), W (4*a*) (0,0,0) and O (24*e*) ($x = 0.24$,0,0). Results are given in Table 1(*a*), which confirm the results of a preliminary study (Baldinozzi *et al.*, 1993): (i) no evidence of substitutional Mg/W disorder is found; (ii) Pb and O thermal motion parameters are large. In the cubic phase of PCW, this point has been explained by a local atomic disorder of Pb and O atoms (Baldinozzi, Sciau & Lapasset, 1992). In a second step, the Pb and O atoms have been assumed to be in a multi-minimum potential around their special positions: O atoms have been distributed on rings lying in the planes orthogonal to the Mg—O—W direction. For Pb, three types of displacement have been tested, along <100>, <110> and <111> directions, leading to 6, 12 and 4 local disorder positions, respectively. The shift of the O atoms gives a noticeable lowering of the *R*-factors (Table 1*b*). For the Pb atoms, the differences between the three types of displacements are very weak and there is a strong correlation between thermal motion and positional disorder (Table 1). A shift is probable, as in the PCW structure, but it is difficult to specify the direction. It can be outlined that the largest Pb shift and the smallest thermal motion are obtained for displacement along the <110> direction.

Structure of the orthorhombic phase

In a preliminary study (Baldinozzi *et al.*, 1993), two space groups were proposed: *Pmcn* (*Pnma*) and $P2_1cn$ ($Pna2_1$). The refinements were only performed in the

* The numbered intensity of each measured point on the profile has been deposited with the IUCr (Reference: DU0393). Copies may be obtained through The Managing Editor, International Union of Crystallography, 5 Abbey Square, Chester CH1 2HU, England.

Table 2. *Results of refinement in the orthorhombic phase*

	294 K				80 K			
	x	*y*	*z*	*B* (Å^2)	*x*	*y*	*z*	*B* (Å^2)
Pb	0.0032 (4)	−0.2196 (2)	0.1422 (1)	1.51 (2)	0.0062 (2)	−0.2113 (2)	0.1464 (1)	0.34 (2)
Mg	0.25	0.7519 (9)	0.3772 (4)	0.44 (4)	0.25	0.7537 (6)	0.3780 (3)	0.21 (4)
W	0.25	0.2577 (6)	0.1161 (2)	0.66 (3)	0.25	0.2569 (5)	0.1136 (2)	0.34 (3)
O(1)	0.4907 (4)	0.2365 (4)	0.1314 (2)	1.09 (3)	0.4910 (3)	0.2298 (3)	0.1340 (2)	0.51 (3)
O(2)	0.25	0.0133 (12)	0.0027 (6)	1.06 (3)	0.25	0.0135 (8)	0.0032 (5)	0.53 (2)
O(3)	0.25	0.4991 (17)	0.0103 (5)	1.06 (3)	0.25	0.4974 (11)	0.0097 (3)	0.53 (2)
O(4)	0.25	−0.0153 (15)	0.2370 (4)	1.06 (3)	0.25	−0.0253 (9)	0.2359 (3)	0.53 (2)
O(5)	0.25	0.4745 (15)	0.2491 (5)	1.06 (3)	0.25	0.4629 (9)	0.2514 (3)	0.53 (2)
$R-F(X)$	$R_{wp}=8.5$	$R_{wp-c}=24.3$	$R_B=9.2$		$R_{wp}=7.4$	$R_{wp-c}=17.7$	$R_B=8.4$	
$R-F(N)$	$R_{wp}=4.0$	$R_{wp-c}=7.2$	$R_B=4.0$		$R_{wp}=4.0$	$R_{wp-c}=7.5$	$R_B=2.9$	

centrosymmetric group (*Pmcn*) with a rigid octahedral block centered on tungsten. Using these results, we have refined the structure in both groups at 294 and 80 K. The final atomic coordinates and temperature factors are listed in Table 2. Refinement in the space group $P2_1cn$ gave no further improvement and so as far as our measurements are concerned, we may consider the structure to be centrosymmetric. The observed diffraction profile and the fit difference for the refinement at 80 K are shown in Fig. 1. Figs. 2 and 3 show the structure in the two phases.

Discussion and concluding remarks

In the cubic phase, the Pb and O atoms are displaced from ideal perovskite positions. Similar results were found in the cubic phase of $BaTiO_3$ (Itoh, Zeng, Nakamura & Mishima, 1985), $PbMg_{1/3}Nb_{2/3}O_3$ (Verbaere, Piffard, Yé & Husson, 1992) and PCW (Baldinozzi *et al.*, 1992). The shifts are larger than those of $BaTiO_3$, but are a little smaller than the shifts found in the two lead perovskites, which could be due to the difference in cell parameters.

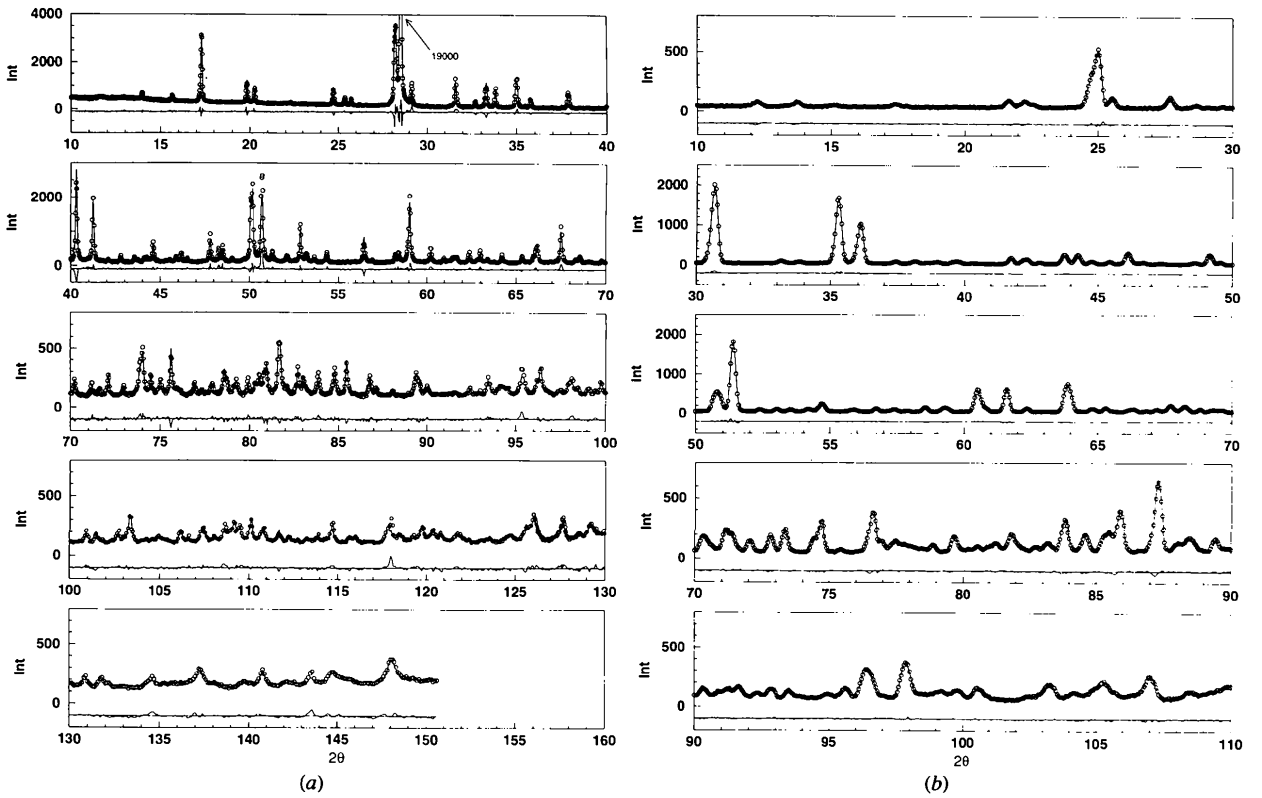

Fig. 1. (*a*) X-ray and (*b*) neutron diffraction powder patterns with the fit difference at 80 K (o experimental, – fit difference).

From Table 2, it is found that the Pb main displacement in the orthorhombic phase from the ideal cubic positions is almost along the $[012]_o$ direction (or $[010]_p$ in the pseudocubic cell). The normal component along the $[100]_o$ direction is very small: 0.05 along $[100]_o$ for 0.33 Å along $[012]_o$ at 80 K. At room temperature, this displacement is to be compared with the disordered displacement of the cubic phase (Table 1*c* or *d*). It is compatible with the hypothesis of an order–disorder phase transition. Pb moves near to O(4) and, to a lesser degree, to $O(1^v)$, $O(1^{vi})$ and $O(5^v)$ (Table 3). The four O atoms build up the base of a pyramid where Pb occupies the top. This layout is close to the PbO_4 pyramid of a PbO structure (Boher, Garnier, Gavarri & Hewat), where, however, the Pb—O distances are smaller (2.34 Å).

At the transition, the octahedra weakly tilt around the $[100]_o$ direction. However, the main O displacements correspond to a weak distortion of the octahedra. O(4), O(5) and O(1) move towards the Pb atoms, while O(2) and O(3) are not shifted. The W and Mg atoms leave the octahedron center. They are shifted in a direction close to $[012]_o$.

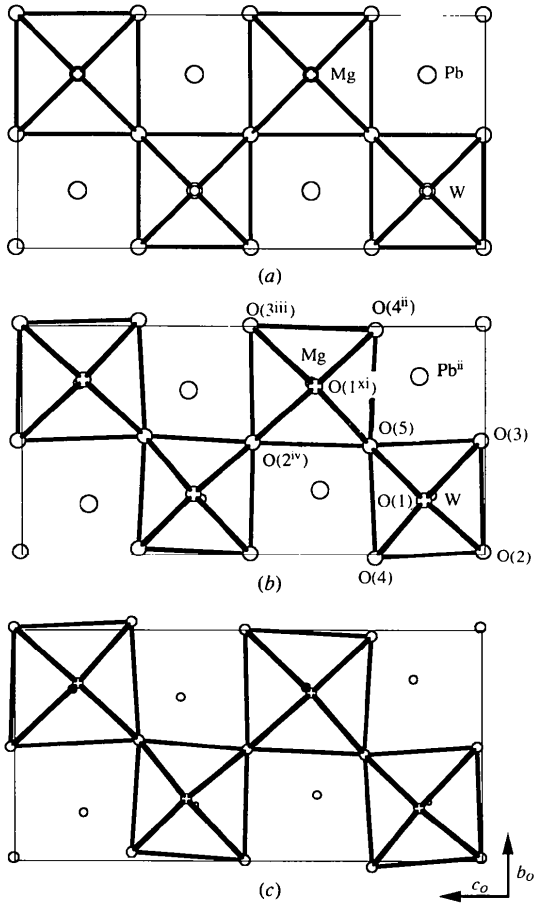

Fig. 2. The structure of PMW on $(100)_o$: (*a*) in the cubic phase, and (*b*) and (*c*) in the orthorhombic phase at 294 and 80 K, respectively.

The antiferroelectric phase of PMW is sometimes compared with that of $PbZrO_3$ (PZ), which is a perovskite with one type of cation on site *B* (Choo *et al.*, 1993). The two phases are orthorhombic with an equivalent cell (Fujishita, Shiozaki, Achiwa & Sawaguchi, 1982; Glazer, Roleder & Dec, 1993). The space group of PZ (*Pbam* or *Pmcb* in our setting) differs from that of PMW by the glide plane normal to the *c*-axis. From symmetry considerations, there are two possible choices for the cell origin: either the Pb or the Zr atoms lie on the mirror plane. The structural determination has shown that this mirror plane is occupied by Pb (Fujishita *et al.*, 1982; Glazer *et al.*, 1993). In the case of the PMW structure, there are two types of octahedra and only the *B* cations (*i.e.* Mg and W) can be on the mirror plane. This position of the mirror plane is not compatible with the tilt of the octahedra observed in the PZ structure and described by the tilt scheme $a^-a^-c^0$ of Glazer (1972, 1975). The octahedral distortions are also similar, but in the case of PMW, it is no more possible to define any significant rigid-body rotation (Figs. 2 and 3).

The symmetries of the Pb displacements in the orthorhombic phases of PZ and PMW are also different. In the first case, we observe only antiparallel shifts in the $[110]_p$ direction; in the second case, there are two symmetry-related types of antiparallel shifts close to the

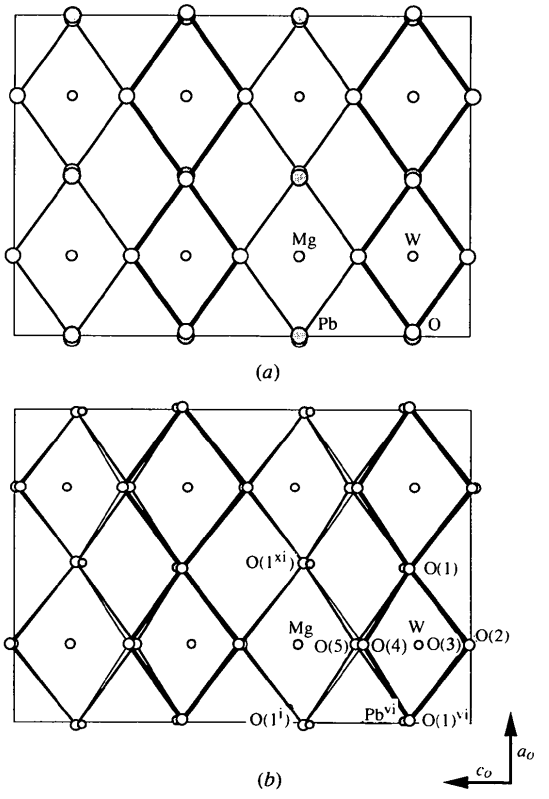

Fig. 3. The structrure of PMW on $(010)_o$: (*a*) in the cubic phase and (*b*) in the orthorhombic phase at 80 K.

Table 3. *Interatomic distances* (Å) *and angles* (°) *with e.s.d.'s in parentheses in the orthorhombic phase*

	294 K	80 K		294 K	80 K
Mg—O(1^{i})	2.064 (3)	2.056 (2)	W—O(3)	1.828 (9)	1.815 (6)
Mg—O(4^{ii})	2.076 (8)	2.058 (5)	W—O(2)	1.899 (8)	1.877 (6)
Mg—O(3^{iii})	2.076 (9)	2.070 (6)	W—O(1)	1.924 (3)	1.925 (2)
Mg—O(2^{iv})	2.079 (8)	2.092 (6)	W—O(5)	1.955 (8)	1.967 (5)
Mg—O(5)	2.150 (9)	2.202 (6)	W—O(4)	2.076 (8)	2.133 (5)
Pb—O(4)	2.522 (5)	2.427 (3)	Pb—O(5^{viii})	2.891 (6)	2.934 (4)
Pb—O(1^{v})	2.596 (3)	2.538 (2)	Pb—O(3^{viii})	2.944 (6)	2.987 (4)
Pb—O(1^{vi})	2.597 (3)	2.520 (2)	Pb—O(4^{ix})	2.962 (6)	3.020 (4)
Pb—O(5^{v})	2.608 (5)	3.541 (3)	Pb—O(3^{vii})	3.098 (6)	3.155 (4)
Pb—O(2)	2.851 (5)	2.836 (4)	Pb—O(1^{x})	3.096 (3)	3.191 (2)
Pb—O(2^{vii})	2.855 (5)	2.882 (4)	Pb—O(1^{vii})	3.124 (3)	3.213 (3)
O(1)—O(4)	2.675 (6)	2.666 (4)	O(1^{i})—O(5)	2.885 (6)	2.868 (4)
O(1)—O(5)	2.700 (6)	2.684 (4)	O(1^{i})—O(4^{ii})	2.913 (6)	2.891 (4)
O(1)—O(2)	2.724 (6)	2.719 (4)	O(1^{i})—O(2^{iv})	2.933 (6)	2.929 (4)
O(1)—O(3)	2.792 (7)	2.825 (4)	O(1^{i})—O(3^{iii})	3.019 (6)	3.052 (4)
O(2)—O(3)	2.764 (12)	2.761 (8)	O(2^{iv})—O(5)	2.893 (9)	2.885 (7)
O(2)—O(4)	2.677 (8)	2.672 (7)	O(2^{iv})—O(3^{iii})	2.925 (12)	2.945 (8)
O(3)—O(5)	2.727 (8)	2.773 (5)	O(3^{iii})—O(4^{ii})	3.119 (7)	3.137 (5)
O(4)—O(5)	2.789 (12)	2.790 (7)	O(4^{ii})—O(5)	2.905 (12)	2.924 (7)
O(1^{i})—Mg—O(1^{xi})	172.7 (3)	169.2 (3)	O(1)—W—O(1^{vi})	167.3 (3)	163.3 (2)
O(1^{i})—Mg—O(2^{iv})	90.1 (2)	89.9 (2)	O(1)—W—O(2)	90.9 (2)	91.3 (1)
O(1^{i})—Mg—O(3^{iii})	93.7 (2)	95.4 (2)	O(1)—W—O(3)	96.1 (2)	98.1 (1)
O(1^{i})—Mg—O(4^{ii})	89.5 (2)	89.3 (2)	O(1)—W—O(4)	83.9 (2)	81.9 (1)
O(1^{i})—Mg—O(5)	86.4 (2)	84.6 (2)	O(1)—W—O(5)	88.2 (2)	87.2 (1)
O(2^{iv})—Mg—O(3^{iii})	89.5 (4)	90.1 (3)	O(2)—W—O(3)	95.7 (4)	96.8 (3)
O(2^{iv})—Mg—O(4^{ii})	173.1 (4)	171.0 (3)	O(2)—W—O(4)	84.6 (4)	83.3 (3)
O(2^{iv})—Mg—O(5)	86.3 (4)	84.4 (3)	O(2)—W—O(5)	172.0 (4)	169.0 (3)
O(3^{iii})—Mg—O(4^{ii})	97.4 (4)	98.9 (3)	O(3)—W—O(4)	179.7 (4)	179.9 (3)
O(3^{iii})—Mg—O(5)	175.8 (4)	174.4 (3)	O(3)—W—O(5)	92.2 (4)	94.2 (3)
O(4^{ii})—Mg—O(5)	86.8 (4)	86.6 (2)	O(4)—W—O(5)	87.5 (3)	85.7 (2)
O(1^{v})—Pb—O(1^{vi})	98.3 (1)	100.9 (1)	O(1^{vi})—Pb—O(4)	63.0 (2)	65.2 (2)
O(1^{v})—Pb—O(4)	69.4 (2)	71.2 (1)	O(1^{vi})—Pb—O(5^{v})	67.3 (2)	69.1 (2)
O(1^{v})—Pb—O(5^{v})	62.5 (2)	63.8 (1)	O(4)—Pb—O(5^{v})	101.6 (2)	105.5 (2)

Symmetry code: (i) $x-\frac{1}{2}, y+\frac{1}{2}, -z+\frac{1}{2}$; (ii) $x, y+1, z$; (iii) $x, -y+\frac{3}{2}, z+\frac{1}{2}$; (iv) $x, -y+\frac{1}{2}, z+\frac{1}{2}$; (v) $x-\frac{1}{2}, y-\frac{1}{2}, -z+\frac{1}{2}$; (vi) $-x+\frac{1}{2}, y, z$; (vii) $x-\frac{1}{2}, -y, -z$; (viii) $x, y-1, z$; (ix) $-x, y-\frac{1}{2}, -z+\frac{1}{2}$; (x) $-x+\frac{1}{2}, y-1, z$; (xi) $-x+1, y+\frac{1}{2}, -z+\frac{1}{2}$.

$[100]_p$ and $[010]_p$ directions (Fig. 4). The magnitudes of these displacements are a little smaller in PMW structure [0.263 (1) and 0.333 (1) Å at 294 and 80 K, respectively]; this difference is to be related to the difference of cell parameters. Nevertheless, the Pb—O distances are of the same order. They vary from 2.427 to 3.213, 2.522 to 3.124 and 2.45 to 3.44 Å in PMW at 80 and 294 K, and in PZ (Fujishita *et al.*, 1982), respectively.

The atom displacements in the antiferroelectric phase of PZ are associated with the Σ_3 mode of the wavevector q_Σ: $(\frac{1}{4},\frac{1}{4},0)$,* and with the R_{25} mode of the wavevector q_R: $(\frac{1}{2},\frac{1}{2},\frac{1}{2})$ (Fujishita & Hoshino, 1984). The second wavevector does not imply any Pb displacement. As far as Pb atoms are concerned, only the first mode has to be considered in this first case. In the case of PMW, as mentioned by Choo *et al.* (1993), the diffraction peaks may be indexed with the two modulation wavevectors q_Σ: $(0,\frac{1}{2},\frac{1}{2})$ and q_X: (1,0,0). A mode analysis (to be published) shows that the atomic displacements can be described by a sum of modulations associated with the lattice vibrational modes Σ_3 of the wavevector q_Σ: $(0,\frac{1}{2},\frac{1}{2})$ and with the mode X_{10} of the wavevector q_X: (1,0,0). These two modes are responsible for different Pb displacement components with different periodicities and are well compatible with the refined displacements.

These two types of modulation wavevectors are also present in the case of the low-temperature phase III of PCW. This allows us to suppose that the Pb displacements in this last compound are analogous to those of PMW. This is confirmed by a recent simulation of convergent-beam electron diffraction results on PCW samples which could be interpretated on the basis of

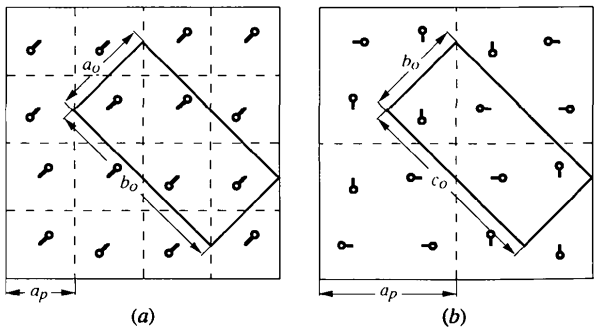

Fig. 4. Schematic diagram showing Pb displacements in the orthorhombic phase of (*a*) PZ from Glazer *et al.* (1993) and (*b*) PMW as viewed on (100). Both pseudocubic and conventional unit cells are displayed.

* The $(\frac{1}{4},\frac{1}{4},0)$ wavevector in PZ becomes equivalent to $(\frac{1}{2},\frac{1}{2},0)$ in the ordered PMW because of the doubling of the prototype cell.

PMW structure (Baldinozzi, Sciau, Buffat & Stadelmann, 1994).

References

BALDINOZZI, G., SCIAU, PH. & BUFFAT, P.-A. (1993). *Solid State Commun.* **86**, 541–544.

BALDINOZZI, G., SCIAU, PH., BUFFAT, P.-A. & STADELMANN, P.-A. (1994). Electron Microscopy ICEM 13 Paris (Les Editions de Physique, Les Ulis), Vol. 1, pp. 875–876.

BALDINOZZI, G., SCIAU, PH. & LAPASSET, J. (1992). *Phys. Status Solidus A*, **133**, 17–23.

BÉRAR, J.-F. & GARNIER, P. (1992), APD 2nd Conference NIST, May 1992, Gaithersburg, Maryland, USA.

BOHER, P., GARNIER, P., GAVARRI, J. R. & HEWAT, A. W. (1985). *J. Solid State Chem.* **57**, 343–350.

CHOO, W. K., KIM, H. J., YANG, J. H., LIM, H., LEE, J. Y., KWON, J. R. & CHUN, C. H. (1993). *Jpn. J. Appl. Phys.* **32**, 4249–4253.

FUJISHITA, H. & HOSHINO, S. (1984). *J. Phys. Soc. Jpn*, **53**, 226–234.

FUJISHITA, H., SHIOZAKI, Y., ACHIWA, N. & SAWAGUCHI, E. (1982). *J. Phys. Soc. Jpn*, **51**, 3583–3591.

GALASSO, F. S. (1990). *Perovskites and High T_c Superconductors*. New York: Gordon and Breach.

GLAZER, A. M (1972). *Acta Cryst.* B**28**, 3384–3392.

GLAZER, A. M (1975). *Acta Cryst.* A**31**, 756–762.

GLAZER, A. M., ROLEDER, K. & DEC, J. (1993). *Acta Cryst.* B**49**, 846–852.

ITOH, K., ZENG, L. Z., NAKAMURA, E. & MISHIMA, N. (1985). *Ferroelectrics*, **63**, 29–37.

LEE, M. H. & CHOO, W. K. (1981). *J. Appl. Phys.* **52**, 5767–5773.

SMOLENSKII, G. A., KRAINIK, N. N. & AGRANOVSKAYA, A. I. (1961). *Fiz. Tverd. Tela*, **3**, 981–990 (*Sov. Phys. Solid State*, **3**, 714–720).

TOKMYANINA, T. B., RAZUMOVSKAYA, O. N. & BELYAEV, I. N. (1976). *Izv. Akad. Nauk SSSR Neorg. Mater.* **12**, 2099–2100.

UCHINO, K. & NOMURA, S. (1976). *J. Phys. Soc. Jpn*, **41**, 542–547.

VERBAERE, A., PIFFARD, Y., YÉ, Z. G. & HUSSON, E. (1992). *Mater. Res. Bull.* **27**, 1227–1234.

Acta Cryst. (1995). B**51**, 673–680

Structure of $Na_3YSi_6O_{15}$ – a Unique Silicate Based on Discrete Si_6O_{15} Units, and a Possible Fast-Ion Conductor

BY S. M. HAILE* AND J. MAIER

Max-Planck-Institute für Festkörperforschung, D-70569 Stuttgart, Germany

B. J. WUENSCH

Department of Materials Science and Engineering, Massachusetts Institute of Technology, Cambridge, MA 02139-4307, USA

AND R. A. LAUDISE

AT&T Bell Laboratories, Murray Hill, NJ 07974-0636, USA

(*Received* 25 *July* 1994; *accepted* 5 *December* 1994)

Abstract

Hydrothermal investigations in the high silica region of the Na_2O–Y_2O_3–Si_6O_{15} system, carried out in a search for novel fast-ion conductors (FIC's), yielded the new compound trisodium yttrium hexasilicate, $Na_3YSi_6O_{15}$. Single-crystal X-ray methods revealed that $Na_3YSi_6O_{15}$ crystallizes in space group *Ibmm*, has lattice constants a = 10.468 (2), b = 15.2467 (13) and c = 8.3855 (6) Å, Z = 4, and 11 atoms in the asymmetric unit. Refinement was carried out to a weighted residual of 3.53% using anisotropic temperature factors for all atoms. The structure is unique in that the silica tetrahedra form isolated $Si_6O_{15}^{6-}$ double dreier-rings, rather than layers as might be expected from the Si to O ratio of 0.4. No isomorphs to $Na_3YSi_6O_{15}$ have been reported.

* Author to whom correspondence should be addressed. Presently at: University of Washington, Department of Materials Science and Engineering, Seattle, WA 98102, USA.

Introduction

High ionic conductivity has been observed in a number of alkali silicates. These include $Na_5YSi_4O_{12}$ (Shannon, Taylor, Gier, Chen & Berzins, 1978), Na_2ZnSiO_4 (Frostäng, Grins & Nygren, 1988), and the solid solution series $Na_{1+x}Zr_2Si_xP_{3-x}O_{12}$ [NASICON (Goodenough, Hong & Kafalas, 1976)]. In such materials, the alkali ion typically migrates *via* channels present in the silicate framework. The transport properties of alkali silicates are amenable to crystal-chemical tailoring because both the tunnel geometry and the size of the mobile ion can be altered *via* substitutions on the non-Si cation sites. Additionally, as with other ionic materials, the concentration of ionic defects can be modified *via* aliovalent substitutions, with the prospect of increasing the ionic conductivity. We were especially interested in $Na_3YSi_6O_{15}$ for a number of reasons. Firstly, we previously measured the conductivity of $K_3NdSi_6O_{15}$ (Haile, Wuensch, Siegrist & Laudise, 1992) and found